

The Relation between The Radius and Mass of The White Dwarf Star at The Extremely Relativistic and Finite-Temperature Case

Ting-Hang Pei

Thpei142857@gmail.com

Abstract In this research, first considering the electron-electron interaction in the high-density Fermi electron gas at $T=0$ K, this interaction causes the pressure $2/137$ time less than the original value. However, the pressure of the Fermi electron gas should have something to do with temperature. Then we estimate the temperature effect using statistical mechanics and find the complicated form of the pressure depends on temperature at the given particle number N and volume V . According to this, the central density-mass, central density-radius, and mass-radius relations of the white dwarf star are obtained by considering the equation of state (EOS). In our calculations, the central density is divided into the high-, middle-, and low-density regions. All three relations are almost unchanged until 10^8 K in the high-density region. The temperature effect mainly affects the middle- and low-density regions and it becomes explicitly above 10^7 K. Our calculations can explain Sloan Digital Sky Survey observations where some white dwarf stars with the radius more than 8×10^3 km have larger mass than the predictions by the relativistic EOS at $T=0$ K. This result tells us that the temperature effect is important for the low and middle central-density white dwarf star and also useful to estimate the inner temperature of a white dwarf star.

Keywords: white dwarf star, degenerate Fermi electron gas, pressure, upper mass limit, electron-electron interaction

I. Introduction

The white dwarf star has been investigated many years and it was named first in 1922 [1]. It usually has very high density with the mass similar to our sun but the volume small like Earth. The reported largest mass seems to be the one found in 2007 which is 1.33 times as large as the solar mass M_{\odot} [2]. The white dwarf star is thought to be the type of the low to medium mass stars in the final evolution stage [3-6]. The early theory to explain its mass upper limit is based on the ideally degenerate Fermi electron gas [6-11]. The calculation adopts all electrons like free particles occupying all energy levels until Fermi energy as they are at zero temperature [12]. It is doubtful that even in the high-temperature and high-pressure situation, the ideal Fermi gas still works. It makes the curiosity further discuss the temperature effect by statistical mechanics.

Actually, the central temperature of the Fermi electron gas in the white dwarf star might be about 10^7 K to 10^8 K [13], the temperature effect should be further considered to get more accurate results. According to statistical mechanics, we first build the pressure produced by the Fermi electron gas at given temperature T , the number of electrons N , and the total volume V . Then we discuss the temperature effect on the

electron pressure. Next, the relations between the central density ρ_c , mass M , and radius R of the white dwarf star are derived from equation of state (EOS). Finally, based on these relations, the temperature effect is discussed and the results are compared to the Sloan Digital Sky Survey (SDSS) observations.

II. The Degenerate Fermi Electron Gas For The White Dwarf Star

First of all, we review the calculation of the upper mass limit for the white dwarf star. It adopts the ideally degenerate Fermi electron gas and considers the relativistic kinetic energy in the calculation [8,9]. Because the electron has spin $s = \pm \frac{1}{2}$, each energy state permits two electrons occupied. Each electron has the rest mass m_e , and its relativistic kinetic energy E_k at momentum p is

$$E_k = m_e c^2 \left\{ \left[1 + \left(\frac{\vec{p}}{m_e c} \right)^2 \right]^{1/2} - 1 \right\}. \quad (1)$$

The Fermi electron gas with the total number N and total volume V has total kinetic energy

$$\begin{aligned} E_0 &= 2m_e c^2 \sum_{|\vec{p}| < p_F} \left\{ \left[1 + \left(\frac{\vec{p}}{m_e c} \right)^2 \right]^{1/2} - 1 \right\} \\ &= \frac{2V m_e c^2}{h^3} \int_0^{p_F} dp 4\pi p^2 \left\{ \left[1 + \left(\frac{\vec{p}}{m_e c} \right)^2 \right]^{1/2} - 1 \right\}, \end{aligned} \quad (2)$$

where h is the Planck's constant and p_F is the Fermi momentum defined as

$$p_F = h \left(\frac{3N}{8\pi V} \right)^{1/3}. \quad (3)$$

Considering the mass m_p of a proton and the mass m_n of a neutron, the total mass M of a white dwarf star mainly consisting of helium nuclei is

$$M = (m_e + m_p + m_n)N \approx 2m_p N \approx 2m_n N. \quad (4)$$

If we define the parameter

$$x_F \equiv \frac{p_F}{m_e c} = \frac{h}{2m_e c} \left(\frac{3N}{8\pi V} \right)^{1/3}, \quad (5)$$

then Eq. (2) becomes

$$E_0 = \frac{8\pi m_e^4 c^5 V}{h^3} \left[f(x_F) - \frac{1}{3} x_F^3 \right], \quad (6)$$

where

$$f(x_F) = \int_0^{x_F} dx x^2 [(1+x^2)^{1/2}]. \quad (7)$$

The pressure produced by the ideal Fermi electron gas is [8]

$$P_0 = -\frac{\partial E_0}{\partial V} = \frac{8\pi m_e^4 c^5}{h^3} \left[\frac{1}{3} x_F^3 \sqrt{1+x_F^2} - f(x_F) \right]. \quad (8)$$

It is almost 1000 times larger than the pressure of the helium nuclei [9]. Further discussions give the relation between the radius R and mass M of the star for the relativistically high-density Fermi electron gas

$$\bar{R} = \bar{M}^{2/3} \left[1 - \left(\frac{\bar{M}}{\bar{M}_0} \right)^{2/3} \right]^{1/2}, \quad (9)$$

where

$$\bar{R} = \left(\frac{2\pi m_e c}{h} \right) R, \quad (10)$$

$$\bar{M} = \frac{9\pi}{8} \frac{M}{m_n}, \quad (11)$$

and

$$\bar{M}_0 = \left(\frac{27\pi}{64\delta} \right)^{3/2} \left(\frac{hc}{2\pi G m_n^2} \right)^{3/2}. \quad (12)$$

In Eq. (12), G is the gravitational constant and δ is a parameter of pure number. Some considerations [9] give the upper mass limit M_0 in unit of the mass M_\odot of our sun

$$M_0 \approx 1.44 M_\odot, \quad (13)$$

which is also the upper limit for appearance of the white dwarf star at $T=0$ K.

III. The Correction of The Electron-Electron Interaction For The White Dwarf Star

The ideally Fermi electron gas has been widely discussed in solid state physics. The ground state energy of non-relativistically high-density Fermi electron gas has been calculated by the Hartree-Fock approximation [14,15] and the energy per electron at

$T=0$ is

$$\frac{E_{HF}}{N} = \frac{2.21}{r_s^2} - \frac{0.916}{r_s} + 0.0622 \ln r_s - 0.096 \left(\frac{\text{Redberg}}{\text{electron}} \right), \quad (14)$$

where E_{HF} is the total energy of the Fermi electron gas, and r_s is defined by using the Bohr radius a_B

$$\frac{V}{N} = \frac{4}{3} \pi r_s^3 a_B^3. \quad (15)$$

The first two terms are dominate terms and the ratio of the first term to the second one is proportional r_s or $N^{1/3}$. As N increases, the first term increases faster than the second one. Actually, the calculation of the first term at the right-hand side in Eq. (14) should use Eq. (6) because of the relativistic electrons. Considering $x_F \gg 1$ in the relativistic region, then Eq. (6) becomes

$$\frac{E_0}{N} \approx \frac{2\pi m_e^4 c^5}{h^3} \frac{V}{N} x_F^4 \left(1 - \frac{4}{3x_F} + \frac{1}{x_F^2} \right). \quad (16)$$

The second term consider the Feynman diagram of the oyster type, so this correlation energy E_1 is [14,15]

$$\begin{aligned} \frac{E_1}{N} &= -\frac{2}{N} \times \frac{1}{2} \times \left[\frac{V}{(2\pi)^3} \right]^2 \times \frac{4\pi K_e e^2}{V} \times \frac{16\pi^4}{h^4} \iint_{\vec{p}_1, \vec{p}_2=0}^{\vec{p}_F} \frac{d^3 \vec{p}_1 d^3 \vec{p}_2}{|\vec{p}_1 - \vec{p}_2|^2} \\ &= -\frac{3}{2\pi} \left(\frac{2\pi K_e p_F a_B}{h} \right) \left(\frac{e^2}{2a_B} \right) = -\frac{3m_e c K_e e^2}{2h} x_F, \end{aligned} \quad (17)$$

where K_e is the Coulomb's constant. Using Eqs. (16) and (17), the pressure P_{HF} of the Fermi electron gas at $T=0$ K is

$$\begin{aligned} P_{HF} &= -\frac{\partial E_{HF}}{\partial V} \\ &= \frac{2\pi m_e^4 c^5}{3h^3} \left(x_F^4 - x_F^2 - 2 \frac{2\pi K_e e^2}{hc} x_F^4 \right) \approx \frac{2\pi m_e^4 c^5}{3h^3} \left(x_F^4 - x_F^2 - \frac{2}{137} x_F^4 \right), \end{aligned} \quad (18)$$

where $2\pi K_e e^2/hc$ is the fine structure constant [16-19]. It means that the electron-electron interaction causes the pressure about 2/137 time less than the original value. Some related discussions can be checked in the early reference [20].

IV. The Temperature Effect On The Pressure of The Ideal Fermi Electron Gas

The central temperature of a star is usually about 10^7 K to 10^8 K, and the upper mass

limit in Eq. (13) calculated at $T=0$ should be improved. Otherwise, it cannot reflect how the relation between the radius and mass of the white dwarf star varies with temperature. Then we consider the case for $T \gg 0$, and the grand partition function in statistical mechanics [9] is

$$q(T, V, z) = \ln Z = \sum_k \ln[1 + z \cdot \exp(-\beta E_k)], \quad (19)$$

Where E_k is the kinetic energy, $\beta=1/k_B T$, and $z=\exp(\mu\beta)$ with μ the chemical potential of the Fermi electron gas. Since the energy eigenstates are treated as arbitrarily close to each other in a very large volume, the grand partition function becomes

$$\ln Z = \int_0^\infty dE g(E_k) \ln[1 + z \exp(-\beta E_k)]. \quad (20)$$

Integrating it by parts, then we have [9]

$$\ln Z = g \frac{4\pi V \beta}{h^3} \frac{1}{3} \int_0^\infty p^3 dp \frac{dE_k}{dp} \frac{1}{z^{-1} \exp(\beta E_k) + 1}, \quad (21)$$

where $g=2s+1$ is the degeneracy factor and

$$p^2 = \frac{E_k^2}{c^2} + 2m_e E_k. \quad (22)$$

Substituting Eq. (22) into Eq. (21) and considering Fermi energy $E_F \gg m_e c^2$, it gives

$$\ln Z = g \frac{4\pi V \beta}{3h^3 c^3} \int_0^\infty dE_k \frac{E_k^3 \left[1 + \frac{2m_e c^2}{E_k}\right]^{3/2}}{z^{-1} \exp(\beta E_k) + 1}. \quad (23)$$

Using the Taylor series expansion to the first-order term, then we have

$$\ln Z \approx g \frac{4\pi V}{3h^3 c^3 \beta^3} \int_0^\infty d(\beta E_k) \frac{(\beta E_k)^3 \left[1 + 3 \left(\frac{\beta m_e c^2}{\beta E_k}\right) + 3 \left(\frac{\beta m_e c^2}{\beta E_k}\right)^2\right]}{z^{-1} \exp(\beta E_k) + 1}. \quad (24)$$

Then the integral gives

$\ln Z \approx$

$$g \frac{4\pi V}{3h^3 c^3 \beta^3} \left[\Gamma(4) f_4(z) + 3 \left(\frac{m_e c^2}{k_B T}\right) \Gamma(3) f_3(z) + 3 \left(\frac{m_e c^2}{k_B T}\right)^2 \Gamma(2) f_2(z) \right], \quad (25)$$

where we define the function

$$f_n(z) = \frac{1}{\Gamma(n)} \int_0^\infty d(\beta E_k) \frac{(\beta E_k)^{n-1}}{z^{-1} e^{(\beta E)} + 1}. \quad (26)$$

The corresponding Fermi energy E_F is roughly 20 MeV [8] and $1/(2m_e c^2 \beta) \sim 1/1000$ at 10^7 K. The chemical potential $\mu \sim E_F$ so $z = \exp(\beta \mu) \sim \exp(20000)$. When $z \gg 1$, the approximation of Eq. (26) [9] is

$$f_n(z) \approx \frac{(\ln z)^n}{n!} \left[1 + \frac{\pi^2 (n-1)n}{6 (\ln z)^2} \right], \quad (27)$$

and the ratio of the first term to the second term is about

$$3 \left(\frac{m_e c^2}{k_B T} \right) \frac{\Gamma(3) f_3(z)}{\Gamma(4) f_4(z)} \approx 3 \left(\frac{m_e c^2}{k_B T} \right) \frac{1/3}{(\ln z)/4} \approx \frac{1}{100}. \quad (28)$$

According to the relation $\ln Z = pV/k_B T$, the pressure causing by the Fermi electron gas is

$$P_{electron} \approx$$

$$\frac{8\pi(k_B T)^4}{3h^3 c^3} \left[\Gamma(4) f_4(z) + 3 \left(\frac{m_e c^2}{k_B T} \right) \Gamma(3) f_3(z) + 3 \left(\frac{m_e c^2}{k_B T} \right)^2 \Gamma(2) f_2(z) \right]. \quad (29)$$

Then we calculate the particle number $N(T, V, z)$ using the similar way in statistical mechanics. It gives

$$\begin{aligned} N(T, V, z) &= g \frac{4\pi V}{h^3} \int_0^\infty p^2 dp \frac{1}{z^{-1} \exp(\beta E_k) + 1} \\ &= g \frac{4\pi V}{h^3 c^3} \int_0^\infty dE_k \frac{E_k^2 \left(1 + \frac{2m_e c^2}{E_k} \right)^{1/2} \left(1 + \frac{m_e c^2}{E_k} \right)}{z^{-1} \exp(\beta E_k) + 1}. \end{aligned} \quad (30)$$

Using Taylor series expansion to the first-order term, then we have

$$N(T, V, z) \approx g \frac{4\pi V}{h^3 c^3 \beta^3} \int_0^\infty d(\beta E_k) \frac{(\beta E_k)^2 \left[1 + 2 \left(\frac{\beta m_e c^2}{\beta E_k} \right) + \frac{1}{2} \left(\frac{\beta m_e c^2}{\beta E_k} \right)^2 \right]}{z^{-1} \exp(\beta E_k) + 1}. \quad (31)$$

Further calculation gives

$$N(T, V, z) \approx$$

$$\frac{8\pi V (k_B T)^3}{h^3 c^3} \left[\Gamma(3) f_3(z) + 2 \left(\frac{m_e c^2}{k_B T} \right) \Gamma(2) f_2(z) + \frac{1}{2} \left(\frac{m_e c^2}{k_B T} \right)^2 f_1(z) \right]. \quad (32)$$

Combing Eq. (29) with Eq. (32), it gives the relation between $P_{electron\ gas}$, T , V , and N , that is,

$$P_{electron\ gas} \approx \frac{Nk_B T}{3V} \left[\frac{\Gamma(4)f_4(z) + 3\left(\frac{m_e c^2}{k_B T}\right)\Gamma(3)f_3(z) + 3\left(\frac{m_e c^2}{k_B T}\right)^2 \Gamma(2)f_2(z)}{\Gamma(3)f_3(z) + 2\left(\frac{m_e c^2}{k_B T}\right)\Gamma(2)f_2(z) + \frac{1}{2}\left(\frac{m_e c^2}{k_B T}\right)^2 f_1(z)} \right]. \quad (33)$$

Substituting Eq. (27) into Eq. (33) and further rearrangement gives

$$\begin{aligned} P_{electron\ gas} &\approx \frac{Nk_B T}{3V} \left\{ \frac{\frac{(\ln z)^4}{4} + \left(\frac{m_e c^2}{k_B T}\right)(\ln z)^3 + \left[\frac{3}{4}\left(\frac{m_e c^2}{k_B T}\right)^2 + \frac{\pi^2}{2}\right](\ln z)^2 + \pi^2\left(\frac{m_e c^2}{k_B T}\right)\ln z}{\frac{(\ln z)^3}{3} + \left(\frac{m_e c^2}{k_B T}\right)(\ln z)^2 + \left[\frac{1}{2}\left(\frac{m_e c^2}{k_B T}\right)^2 + \frac{\pi^2}{3}\right]\ln z + \frac{\pi^2}{3}\left(\frac{m_e c^2}{k_B T}\right)} \right\} \\ &\approx \frac{Nk_B T}{4V} (\ln z) \left\{ 1 + \left(\frac{m_e c^2}{k_B T}\right) \frac{1}{\ln z} - \frac{3}{2} \left(\frac{m_e c^2}{k_B T}\right)^2 \frac{1}{(\ln z)^2} + \frac{\pi^2}{(\ln z)^2} \right. \\ &\quad \left. + \left[3 \left(\frac{m_e c^2}{k_B T}\right)^3 - \pi^2 \left(\frac{m_e c^2}{k_B T}\right) \right] \frac{1}{(\ln z)^3} \right\}. \quad (34) \end{aligned}$$

In Eq. (34), $(\ln z)$ can be obtained by substituting Eq. (27) into Eq. (32). Then we have

$$\begin{aligned} \frac{N}{V} &\approx \frac{8\pi(k_B T)^3}{(hc)^3} \times \\ &\left[\frac{(\ln z)^3}{3} + \left(\frac{m_e c^2}{k_B T}\right)(\ln z)^2 + \left[\frac{1}{2}\left(\frac{m_e c^2}{k_B T}\right)^2 + \frac{\pi^2}{3}\right](\ln z) + \frac{\pi^2}{3}\left(\frac{m_e c^2}{k_B T}\right) \right]. \quad (35) \end{aligned}$$

Considering $(\ln z) \gg (m_e c^2/k_B T)$, and using $(\ln z) = \mu/k_B T$ and the definition of the Fermi momentum in Eq. (3), it further gives

$$(cp_F)^3 \approx \left\{ \mu^3 + 3(m_e c^2)\mu^2 + \left[\frac{3}{2}(m_e c^2)^2 + \pi^2(k_B T)^2\right]\mu + \pi^2(m_e c^2)(k_B T)^2 \right\}. \quad (36)$$

Finding the cubic roots at both sides in Eq. (36), and expanding the bracket to the second-order $(1/\mu)$ -term give

$$cp_F \approx \mu \left\{ 1 + \left(\frac{m_e c^2}{\mu}\right) + \left[-\frac{1}{2}(m_e c^2)^2 + \frac{\pi^2}{3}(k_B T)^2 \right] \frac{1}{\mu^2} \right\}. \quad (37)$$

Eq. (37) results in two μ solutions, and we choose the reasonable one

$$\begin{aligned}
\mu &\approx \frac{(cp_F - m_e c^2) + (cp_F - m_e c^2) \left\{ 1 - 2 \left[\frac{-\frac{1}{2}(m_e c^2)^2 + \frac{\pi^2}{3}(k_B T)^2}{(cp_F - m_e c^2)^2} \right] \right\}}{2} \\
&\approx cp_F \left[1 - \left(\frac{m_e c^2}{cp_F} \right) + \frac{1}{2} \left(\frac{m_e c^2}{cp_F} \right)^2 - \frac{\pi^2}{3} \left(\frac{k_B T}{cp_F} \right)^2 \right], \\
&\approx E_F - \frac{\pi^2}{3} (cp_F) \left(\frac{k_B T}{cp_F} \right)^2, \tag{38}
\end{aligned}$$

where the relativistic Fermi energy by using Eq. (1) is defined as

$$E_F \approx cp_F \left[1 - \left(\frac{m_e c^2}{cp_F} \right) + \frac{1}{2} \left(\frac{m_e c^2}{cp_F} \right)^2 \right]. \tag{39}$$

It reasonably reveals that $\mu \rightarrow E_F$ when $T \rightarrow 0$ in Eq. (38). Substituting Eq. (38) into Eq. (34), the pressure of the electron gas in Eq. (34) is

$$\begin{aligned}
P_{electron} &\approx \\
\frac{N}{4V} (cp_F) &\left\{ \left[1 + \frac{1}{2} \left(\frac{m_e c^2}{cp_F} \right)^2 - \frac{\pi^2}{3} \left(\frac{k_B T}{cp_F} \right)^2 \right] \right. \\
&\quad - \frac{\left[\frac{3}{2} - \pi^2 \left(\frac{k_B T}{m_e c^2} \right)^2 \right]}{\left[\left(\frac{cp_F}{m_e c^2} \right)^2 - \left(\frac{cp_F}{m_e c^2} \right) + \frac{1}{2} - \frac{\pi^2}{3} \left(\frac{k_B T}{m_e c^2} \right)^2 \right]} \\
&\quad \left. + \frac{\left[3 - \pi^2 \left(\frac{k_B T}{m_e c^2} \right)^2 \right] \left(\frac{cp_F}{m_e c^2} \right)}{\left[\left(\frac{cp_F}{m_e c^2} \right)^2 - \left(\frac{cp_F}{m_e c^2} \right) + \frac{1}{2} - \frac{\pi^2}{3} \left(\frac{k_B T}{m_e c^2} \right)^2 \right]^2} \right\}. \tag{40}
\end{aligned}$$

It explicitly tells us that the total pressure depends on temperature complicatedly at the given particle number N and volume V . The pressure of the Fermi electron gas in the white dwarf star should have something to do with temperature as we see in Eq. (40).

After obtaining the pressure of the degenerate Fermi electron gas varying with temperature, then we can estimate the relation between mass and radius of the white

dwarf star. The relation between V and R is

$$V = \frac{4}{3}\pi R^3. \quad (41)$$

Using Eqs (4), (10), (11), and (35), it gives [8]

$$\frac{N}{V} \approx \frac{3M}{8\pi m_n R^3} = \left(\frac{3}{8\pi m_n}\right) \left(\frac{8m_n}{9\pi}\right) \left(\frac{2\pi m_e c}{h}\right)^3 \frac{\bar{M}}{\bar{R}^3} = \left(\frac{8\pi m_e^3 c^3}{3h^3}\right) \frac{\bar{M}}{\bar{R}^3}. \quad (42)$$

The equilibrium condition by considering the gravitational self-energy [8] is

$$\frac{1}{4} \left(\frac{8\pi m_e^3 c^3 k_B T}{3h^3} \right) \left\{ (cp_F) \left[1 - \left(\frac{m_e c^2}{cp_F} \right)^2 + \frac{2\pi^2}{3} \left(\frac{k_B T}{cp_F} \right)^2 \right] \right\} \frac{\bar{M}}{\bar{R}^3} = K' \frac{\bar{M}^2}{\bar{R}^4}, \quad (43)$$

where

$$K' = \frac{\delta}{4\pi} G \left(\frac{8m_n}{9\pi} \right)^2 \left(\frac{2\pi m_e c}{h} \right)^4. \quad (44)$$

In Eq. (38), δ is a parameter of pure number and G is the gravitational constant [9]. Substituting Eq. (38) into Eq. (37), then we have

$$\frac{\bar{M}}{\bar{R}} = \frac{1}{4} \left(\frac{27}{64\delta G} \right) \left(\frac{2h}{m_n^2 m_e c} \right) \left\{ \left(\frac{cp_F}{k_B T} \right) \left[1 - \left(\frac{m_e c^2}{cp_F} \right)^2 + \frac{2\pi^2}{3} \left(\frac{k_B T}{cp_F} \right)^2 \right] \right\}. \quad (45)$$

Further arrangement gives

$$\frac{M}{R} \approx \left(\frac{3}{2\delta G m_n} \right) \left\{ \frac{cp_F}{4} \left[1 - \left(\frac{m_e c^2}{cp_F} \right)^2 + \frac{2\pi^2}{3} \left(\frac{k_B T}{cp_F} \right)^2 \right] \right\}. \quad (46)$$

Then we adopt the approximation of $E_F \sim cp_F$ in Eq. (46), and it gives

$$\frac{M}{R} \approx \left(\frac{3}{8\delta G m_n} \right) \left\{ c \left(\frac{3h^3 N}{8\pi V} \right)^{1/3} - \left(\frac{8\pi V}{3h^3 N} \right)^{1/3} \left[(m_e^2 c^3) - \frac{2\pi^2 (k_B T)^2}{3c} \right] \right\}, \quad (47)$$

Substituting Eq. (42) into Eq. (47) and arranging it, then we have

$$\left(\frac{8\delta G m_n}{3c} \right) M^{4/3} \approx$$

$$\left(\frac{9h^3}{64\pi^2 m_n}\right)^{1/3} M^{2/3} - \left(\frac{64\pi^2 m_n}{9h^3}\right)^{1/3} \left[(m_e^2 c^2) - \frac{2\pi^2 (k_B T)^2}{3c^2} \right] R^2. \quad (48)$$

Solving R in Eq. (48) and expanding the square root to the second order, the relation between radius, temperature, and mass is

$$R \approx \frac{1}{m_e c \left[1 - \frac{2\pi^2 (k_B T)^2}{3(m_e c^2)^2} \right]^{1/2}} \left(\frac{9h^3}{64\pi^2 m_n}\right)^{1/3} M^{1/3} \left[1 - \left(\frac{M}{M_0}\right)^{2/3} \right]^{1/2}, \quad (49)$$

where

$$M_0 = \left(\frac{3c}{8\delta G m_n}\right)^{3/2} \left(\frac{9h^3}{64\pi^2 m_n}\right)^{1/2} = \frac{9hc}{64\pi\delta G m_n^2} \left(\frac{3hc}{8\delta G}\right)^{1/2}. \quad (50)$$

M_0 in Eq. (50) is the upper mass limit of the white dwarf star in the extremely relativistic case [8,9]. Eq. (49) is the same result as the case of $p_F \gg m_e c$ at $T=0$ K [8,9]. According to Eq. (49) at $T=0$ K, the radius of the white dwarf star with the solar mass is about 2700 km [9]. The more important thing is the temperature term appear in the numerator of Eq. (49), which is much more reasonable than it is at $T=0$ K. It explicitly tells us that the relation between M and R depends on T , m_n , and m_e .

Then the radius-mass curve described in Eq. (49) at $T=0$ K is drawn in Fig. 1. The upper mass limit M_0 is chosen as $1.44M_\odot$ at $\delta=0.65$ and $M_\odot=1.99 \times 10^{30}$ kg [9,21]. Most early research derived the relation of the radius and mass of the white dwarf star through the equation of state (EOS) [8,9]. However, the result shows the divergence of the radius when mass goes to zero for the low-density white dwarf star [8,9]. As we know, the density of the white dwarf star is about [8,9]

$$\rho \equiv \frac{N}{V} \approx 10^7 \text{ g/cm}^3 \approx 10^{13} \text{ mole/m}^3 \approx 6 \times 10^{36} \text{ electrons/m}^3. \quad (51)$$

When we consider the condition $p_F \gg m_e c$, it means

$$\frac{N}{V} \gg \frac{8\pi(m_e c^2)^3}{3h^3} = 5.2 \times 10^{35} \text{ electrons/m}^3. \quad (52)$$

As long as the white dwarf star possesses the minimal density as shown in Eq. (51), this condition is satisfied. In our common environment on the Earth, the most things have density much lower than that of the white dwarf star in Eq. (51). When thing disappears like the melting ice, its volume also becomes zero. A white dwarf star having very large radius as its mass goes to zero is much unreasonable.

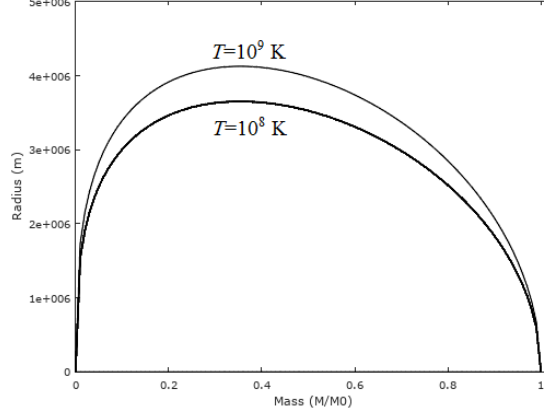


Figure 1. The relation between radius and mass of the white dwarf star by Eq. (49) at the condition $p_F \gg m_e c$ without considering EOS.

The other consideration is about $m_e c^2 \gg E_F$, then the partition function, pressure, and number of the ideal Fermi electron gas become

$$\ln Z \approx g \frac{4\pi V (2m_e)^{3/2}}{3h^3 \beta^{3/2}} \times \left[\Gamma\left(\frac{5}{2}\right) f_{5/2}(z) + \frac{3}{4} \left(\frac{k_B T}{m_e c^2}\right) \Gamma\left(\frac{7}{2}\right) f_{7/2}(z) + \frac{3}{32} \left(\frac{k_B T}{m_e c^2}\right)^2 \Gamma\left(\frac{9}{2}\right) f_{9/2}(z) \right], \quad (53)$$

$$P_{electron\ gas} \approx \frac{8\pi (2m_e)^{3/2} (k_B T)^{5/2}}{3h^3} \left[\Gamma\left(\frac{5}{2}\right) f_{5/2}(z) + \frac{3}{4} \left(\frac{k_B T}{m_e c^2}\right) \Gamma\left(\frac{7}{2}\right) f_{7/2}(z) \right], \quad (54)$$

and

$$N(T, V, z) \approx \frac{4\pi V (2m_e)^{3/2} (k_B T)^{3/2}}{h^3} \times \left[\Gamma\left(\frac{3}{2}\right) f_{3/2}(z) + \frac{5}{4} \left(\frac{1}{m_e c^2 \beta}\right) \Gamma\left(\frac{5}{2}\right) f_{5/2}(z) + \frac{7}{32} \left(\frac{1}{m_e c^2 \beta}\right)^2 \Gamma\left(\frac{7}{2}\right) f_{7/2}(z) \right]. \quad (55)$$

Combing Eq. (55) with Eq. (54), it gives the relationship between $P_{electron\ gas}$, T , V , and N

$$P_{electron\ gas} \approx \frac{2Nk_B T}{3V} \left[\frac{\Gamma\left(\frac{5}{2}\right) f_{5/2}(z) + \frac{3}{4} \left(\frac{k_B T}{m_e c^2}\right) \Gamma\left(\frac{7}{2}\right) f_{7/2}(z) + \frac{3}{32} \left(\frac{k_B T}{m_e c^2}\right)^2 \Gamma\left(\frac{9}{2}\right) f_{9/2}(z)}{\Gamma\left(\frac{3}{2}\right) f_{3/2}(z) + \frac{5}{4} \left(\frac{k_B T}{m_e c^2}\right) \Gamma\left(\frac{5}{2}\right) f_{5/2}(z) + \frac{7}{32} \left(\frac{k_B T}{m_e c^2}\right)^2 \Gamma\left(\frac{7}{2}\right) f_{7/2}(z)} \right]. \quad (56)$$

Here we use the non-relativistic chemical potential for $E_F \gg k_B T$ [4]

$$\mu \approx E_F \left[1 - \frac{\pi^2}{12} \left(\frac{k_B T}{E_F} \right)^2 - \frac{89\pi^4}{25920} \left(\frac{k_B T}{E_F} \right)^4 \right] \quad (57)$$

where

$$E_F \approx \frac{p_F^2}{2m_e} - \frac{p_F^4}{8m_e^3 c^2}. \quad (58)$$

Further rearrangement of Eq. (56) and ignoring T^2 terms in Eq. (56) and T^4 term in Eq. (57) give

$$\begin{aligned} P_{electron\ gas} &\approx \frac{2Nk_B T}{3V} \left[\frac{\Gamma\left(\frac{5}{2}\right) f_{5/2}(z)}{\Gamma\left(\frac{3}{2}\right) f_{3/2}(z)} \right] \left\{ \frac{1 + \frac{3}{4} \left(\frac{k_B T}{m_e c^2} \right) \left[\frac{\Gamma\left(\frac{7}{2}\right) f_{7/2}(z)}{\Gamma\left(\frac{5}{2}\right) f_{5/2}(z)} \right]}{1 + \frac{5}{4} \left(\frac{k_B T}{m_e c^2} \right) \left[\frac{\Gamma\left(\frac{5}{2}\right) f_{5/2}(z)}{\Gamma\left(\frac{3}{2}\right) f_{3/2}(z)} \right]} \right\} \\ &\approx \frac{Nk_B T}{V} \left(\frac{2}{5} \ln z \right) \left[1 - \frac{3}{14} \left(\frac{k_B T}{m_e c^2} \ln z \right) \right] \\ &\approx \frac{N}{V} \left\{ \frac{2}{5} E_F \left[1 - \frac{\pi^2}{12} \left(\frac{k_B T}{E_F} \right)^2 \right] \right\} \left\{ 1 - \frac{3}{14} \left(\frac{E_F}{m_e c^2} \right) \left[1 - \frac{\pi^2}{12} \left(\frac{k_B T}{E_F} \right)^2 \right] \right\}. \quad (59) \end{aligned}$$

After obtaining the pressure of the ideal Fermi electron gas varying with temperature, then we can estimate the relationship between mass and radius of the white dwarf star. The equilibrium condition in Eq. (43) becomes

$$\begin{aligned} &\left(\frac{8\pi m_e^3 c^3}{3h^3} \right) \left\{ \frac{2}{5} E_F \left[1 - \frac{\pi^2}{12} \left(\frac{k_B T}{E_F} \right)^2 \right] \right\} \left\{ 1 - \frac{3}{14} \left(\frac{E_F}{m_e c^2} \right) \left[1 - \frac{\pi^2}{12} \left(\frac{k_B T}{E_F} \right)^2 \right] \right\} \frac{\bar{M}}{\bar{R}^3} \\ &= K' \frac{\bar{M}^2}{\bar{R}^4}, \quad (60) \end{aligned}$$

and it gives

$$M = \left(\frac{3}{2\delta G m_n} \right) \left\{ \frac{2}{5} E_F \left[1 - \frac{\pi^2}{12} \left(\frac{k_B T}{E_F} \right)^2 \right] \right\} \left\{ 1 - \frac{3}{14} \left(\frac{E_F}{m_e c^2} \right) \left[1 - \frac{\pi^2}{12} \left(\frac{k_B T}{E_F} \right)^2 \right] \right\} R. \quad (61)$$

This reasonably shows that the radius disappears as $M \rightarrow 0$ verifying the previous viewpoint.

V. The Mass-Radius Relation Obtained From EOS

Next, we further obtain the some relations from EOS, the equation of equilibrium for the stellar structure [12,22-24]. There are two equations to be considered here:

$$\frac{dP(r)}{dr} = -\frac{Gm(r)\rho(r)}{r^2} \quad (62)$$

and

$$\frac{dm(r)}{dr} = 4\pi r^2 \rho(r), \quad (63)$$

where $P(r)$, $m(r)$, and $\rho(r)$ are the distributions of the pressure, mass, and mass density varying with the radial position in the star, respectively. Theoretically speaking, once the distribution of $\rho(r)$ is known, the distributions of the pressure and mass can be obtained by substituting $\rho(r)$ into Eqs. (62) and (63). The boundary conditions are $m(0)=0$, $\rho(r)=\rho_c$, $m(R)=\rho(R)=0$, and $d\rho(r)/dr=0$ at $r=0$ where ρ_c is the central density. Then defining the parameter

$$x = x_F \equiv \frac{p_F}{m_e c} = \left(\frac{\rho}{\rho_0}\right)^{1/3}, \quad (64)$$

where

$$\rho_0 = 2m_n \left(\frac{8\pi m_e^3 c^3}{3h^3}\right). \quad (65)$$

Using Eq. (64), the high Fermi-energy pressure in Eq. (40) becomes

$P_{electron} \approx$
 $_{gas}$

$$\frac{2\pi m_e^4 c^5}{3h^3} x^4 \left\{ \left[1 + \frac{1}{2} \left(\frac{1}{x}\right)^2 - \frac{\pi^2}{3} \left(\frac{k_B T}{m_e c^2}\right)^2 \left(\frac{1}{x}\right)^2 \right] - \frac{\left[\frac{3}{2} - \pi^2 \left(\frac{k_B T}{m_e c^2}\right)^2 \right]}{\left[x^2 - x + \frac{1}{2} - \frac{\pi^2}{3} \left(\frac{k_B T}{m_e c^2}\right)^2 \right]} \right. \\ \left. + \frac{\left[3 - \pi^2 \left(\frac{k_B T}{m_e c^2}\right)^2 \right] x}{\left[x^2 - x + \frac{1}{2} - \frac{\pi^2}{3} \left(\frac{k_B T}{m_e c^2}\right)^2 \right]^2} \right\}. \quad (66)$$

From Eq. (62), it induces

$$\frac{d\rho}{dr} = -\left(\frac{dP}{d\rho}\right)^{-1} \frac{Gm\rho}{r^2}. \quad (67)$$

Then it is derived

$$\begin{aligned}
\frac{dP}{d\rho} = & \left(\frac{2\pi m_e^4 c^5}{3h^3} \right) \frac{1}{3\rho_0} \left\{ 4x + x - \frac{2\pi^2}{3} \left(\frac{k_B T}{m_e c^2} \right)^2 x \right. \\
& - \left[\frac{3}{2} - \pi^2 \left(\frac{k_B T}{m_e c^2} \right)^2 \right] \frac{4x}{x^2 - x + \frac{1}{2} - \frac{\pi^2}{3} \left(\frac{k_B T}{m_e c^2} \right)^2} \\
& + \left[\frac{3}{2} - \pi^2 \left(\frac{k_B T}{m_e c^2} \right)^2 \right] \frac{x^2(2x-1)}{\left[x^2 - x + \frac{1}{2} - \frac{\pi^2}{3} \left(\frac{k_B T}{m_e c^2} \right)^2 \right]^2} \\
& + \left[3 - \pi^2 \left(\frac{k_B T}{m_e c^2} \right)^2 \right] \frac{5x^2}{\left[x^2 - x + \frac{1}{2} - \frac{\pi^2}{3} \left(\frac{k_B T}{m_e c^2} \right)^2 \right]^2} \\
& \left. - \left[3 - \pi^2 \left(\frac{k_B T}{m_e c^2} \right)^2 \right] \frac{2x^3(2x-1)}{\left[x^2 - x + \frac{1}{2} - \frac{\pi^2}{3} \left(\frac{k_B T}{m_e c^2} \right)^2 \right]^3} \right\}. \quad (68)
\end{aligned}$$

Finally, we can obtain the differential equation of $\rho(r)$ by substituting Eq. (68) into Eq. (67). Similarly, the case for the low Fermi-energy pressure can be obtained by using Eq. (56). For $\mu \geq k_B T$,

$$\begin{aligned}
& \frac{dP}{d\rho} \\
& = \frac{d}{dx} \left\{ \left(\frac{2\pi m_e^4 c^5}{3h^3} \right) \frac{4}{5} \left(x^5 - \frac{x^7}{4} \right) \left[1 - \frac{\pi^2}{3} \left(\frac{k_B T}{m_e c^2} \right)^2 \frac{1}{(x^2 - x^4/4)^2} \right] \right. \\
& \quad \times \frac{\left[y^2 + \frac{5\pi^2}{8} y^4 \right] + \frac{15}{28} \left(\frac{k_B T}{m_e c^2} \right) \left[y + \frac{35\pi^2}{24} y^3 \right] + \frac{1}{48} \left(\frac{k_B T}{m_e c^2} \right)^2 \left[1 + \frac{21\pi^2}{8} y^2 \right]}{\left[y^2 + \frac{\pi^2}{8} y^4 \right] + \frac{3}{4} \left(\frac{k_B T}{m_e c^2} \right) \left[y + \frac{5\pi^2}{8} y^3 \right] + \frac{1}{16} \left(\frac{k_B T}{m_e c^2} \right)^2 \left[1 + \frac{35\pi^2}{24} y^2 \right]} \left. \right\} \frac{dx}{d\rho}, \quad (69)
\end{aligned}$$

where

$$y \equiv \frac{k_B T}{\mu}, \quad (70)$$

and the expression of μ in Eq. (57) is adopted here. Using Eqs. (63) and (67) with the boundary conditions $\rho(0)=\rho_c$, $\rho(R)=0$, and $d\rho/dr=0$ at $r=0$, we can obtain the central density-mass, central density-radius, and mass-radius relations numerically. The

numerical method is the fourth-order Runge-Kutta method [25]. According to the definition of the parameter x in Eq. (64), the calculations are divided into three regions by considering the central mass density ρ_c at different temperature. The temperature of the white dwarf star is considered homogeneously here. The high-density region is for $\rho_c > \rho_0$, and we choose $\rho_c \geq 5 \times 10^{10} \text{ kg/m}^3$ in our high-density calculations by using Eqs. (66) and (68). The low-density region is for $\rho_c < \rho_0$, and we choose $\rho_c \leq 10^9 \text{ kg/m}^3$ in the low-density calculations by using Eqs. (56) and (69). Between 10^9 kg/m^3 and $5 \times 10^{10} \text{ kg/m}^3$ is the middle-density region, where it can be approximated by connecting the high- and low-density regions directly. In Fig. 2(a), the relation between mass and the central density of the white dwarf star is given in the high-, middle-, and low-density regions at different temperature. In the high-density region, the mass is close to $1.4 M_\odot$ after 10^{13} kg/m^3 . Those curves are almost the same one from low temperature to 10^8 K in this region, so only two cases at 10^7 K and 10^8 K are shown. In the low-density region, those curves have tiny deviation until $T = 10^7 \text{ K}$, and especially they are almost coincident at $\rho_c \geq 2 \times 10^7 \text{ kg/m}^3$. At $T = 5 \times 10^7 \text{ K}$, the curve is explicitly changed and the starting point is at $5 \times 10^6 \text{ kg/m}^3$. It means that the white dwarf star at this temperature has the central density higher than $5 \times 10^6 \text{ kg/m}^3$. As temperature increases, the starting point of the central density also increases. It is about 10^7 kg/m^3 at 10^8 K , $4 \times 10^7 \text{ kg/m}^3$ at $2 \times 10^8 \text{ K}$, and $7 \times 10^7 \text{ kg/m}^3$ at $3 \times 10^8 \text{ K}$. In the middle-density region, although the central density is only from 10^9 kg/m^3 to $5 \times 10^{10} \text{ kg/m}^3$, the range of mass covers a large interval from $0.4 M_\odot$ to $1.1 M_\odot$. It means that the large part of the white dwarf stars is located in this region.

In Fig. 2(b), the relation between the central density and mass is given in the high-, middle-, and low-density regions at different temperature. Both axes are shown in log scale. The central density is from 10^5 kg/m^3 to 10^{14} kg/m^3 , and the radius is from 5×10^5 to 5×10^7 . At 10^6 K , it shows a logarithm relation between the central density and the radius of the white dwarf star. The higher central density is, the smaller the radius is. However, the trend is broken at 10^7 K and above. At 10^7 K , there is a turning point around the central density of 10^6 kg/m^3 which means the maximal radius of the white dwarf star at this temperature is less than $3 \times 10^7 \text{ m}$ or $3 \times 10^4 \text{ km}$. This turning point also means that the radius of the white dwarf star cannot increase infinitely as mentioned before. When we the mass goes to zero, the radius also approaches zero. If we extend the curve to zeros radius, it exhibit that the central density is always above 10^5 kg/m^3 at 10^7 K . The turning point increase in the central density as temperature increases, but the maximal radius decreases at the same time. The turning point is roughly 10^7 kg/m^3 at $5 \times 10^7 \text{ K}$ and 10^8 kg/m^3 at $2 \times 10^8 \text{ K}$. In conclusion, the same radius of the white dwarf star would correspond to different central density, and one is in the high-density region and the other is in the low-density region.

In Fig. 2 (c), the mass-radius relation for the white dwarf star is shown. As mentioned in Fig. 2(a), the mass is close to $1.4 M_{\odot}$ after 10^{13} kg/m^3 in the high-density region. Those curves are almost the same one from low temperature to 10^8 K in the high-density region, and only two cases at 10^7 K and 10^8 K are shown in this region. In the low-density region, those curves have tiny deviation until $T=10^7 \text{ K}$, and it is almost coincident at $\rho_c \geq 2 \times 10^7 \text{ kg/m}^3$. In the middle-density region, the range of mass covers a large interval from $0.4 M_{\odot}$ to $1.1 M_{\odot}$ where the central density is only from 10^9 kg/m^3 to $5 \times 10^{10} \text{ kg/m}^3$. It also implies that a large part of the white dwarf star we found astronomically belong to the middle-density region. Those results are the same as Fig. 2(a). Especially, at $T=5 \times 10^7 \text{ K}$ and above, it exists some parts that the mass at the same radius is larger than the curve at 10^7 K and below. Recently, the Sloan Digital Sky Survey Release 4 shows a lot of observations having larger mass comparing to the relativistic EOS at $T=0 \text{ K}$ when the radius is more than $8 \times 10^3 \text{ km}$ [22]. By using our calculations in Fig. 2(c), this phenomenon can be explained because the higher temperature results in these white dwarf stars of larger mass appearing at the same radius in the low-density region. Those parts are denoted by the dotted elliptic curve in Fig. 2(c). This explanation can also extend to the middle region in Fig. 2(c).

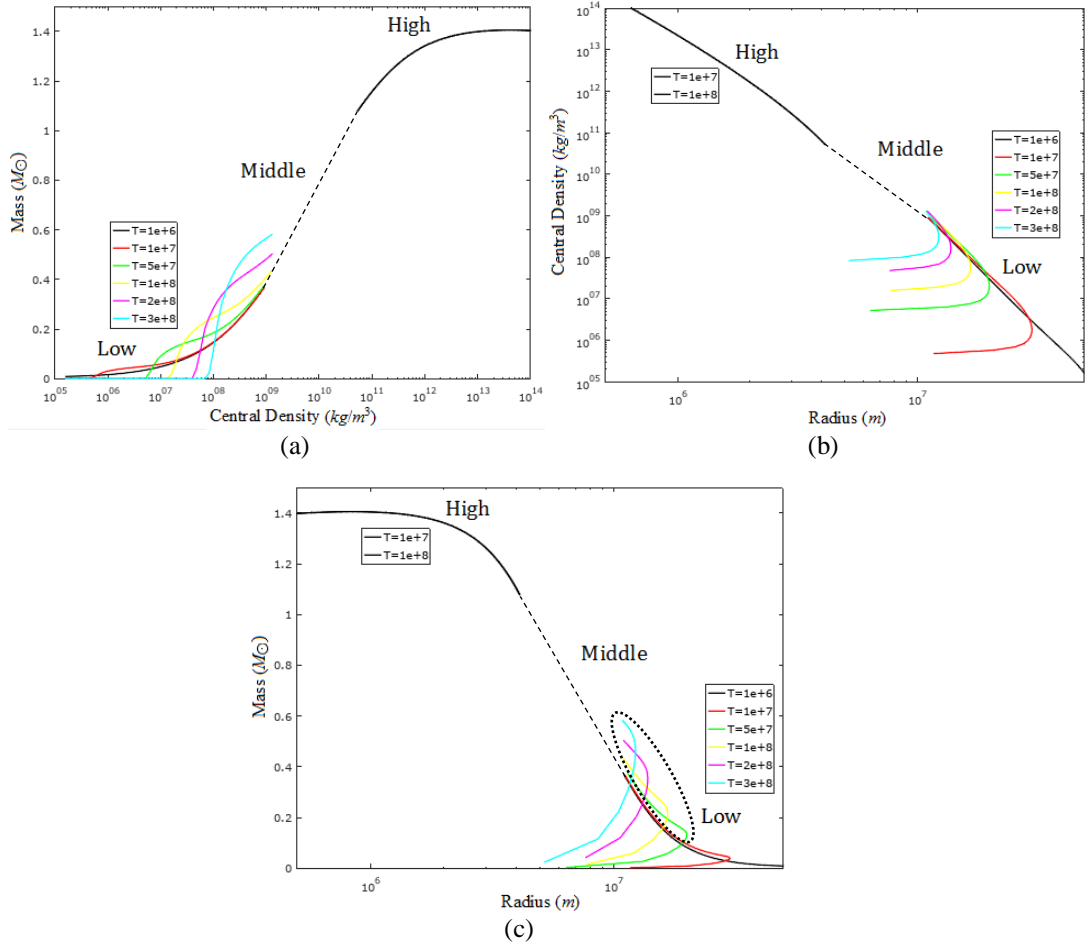


Figure 2. The relations at different temperature in the high-, middle-, and low-density regions between (a) mass and the central density, (b) the central density and radius, and (c) mass and radius.

V. Conclusion

In summary, the mass-radius relation of the white dwarf star derived according to statistical mechanics shows that the temperature effect has to be considered at high temperature above 10^7 K. After all, the ideally degenerate Fermi electron gas is described at $T=0$ K, and the temperature effect would show something difference. The other corrections is due to the electron-electron interaction considered at $T=0$. The calculation considers the relativistic electrons and the result shows that this effect causes the pressure $2/137$ time less than the original value. It means that the many-particle effect appears and causes about 1.5% deviation in pressure. When the temperature effect is considered, the pressure is calculated by statistical mechanics. According to the Fermi energy, two cases are calculated. One is $E_F \gg m_e c^2$, and the other is $E_F \ll m_e c^2$. Because of the temperature effect, the chemical potential is also temperature-dependent and different expression in these two cases. From the deductions, the pressure produced by the Fermi electron gas depends on temperature complicatedly at the given particle number N and volume V . The mass-radius relation of the white dwarf star without considering EOS is obtained for two cases and the radius is zero as the mass of the white dwarf star disappears.

Then, further considering EOS, the central density-mass, the central density-radius, and the mass-radius relations are obtained. The central density is divided into the high-, middle-, and low-density regions where the results can be coincident with the SDSS observations. In the high-density region, three relations are almost unchanged until 10^8 K. The temperature effect mainly affects the low-density region at temperature above 10^7 K. Especially, the mass-radius curves show some parts having larger mass at the same radius when temperature is higher. It gives an away to explain the SDSS observations at the radius more than 8×10^3 km that the mass of the white dwarf star is often larger than the prediction by the relativistic EOS at zero temperature. Those white dwarf stars of larger mass just correspond to the low- and middle-density regions. It means that we should consider the temperature effect to get the better calculations which can reasonably explain the astronomical observations.

Reference:

- [1]. J. B. Holberg, "How Degenerate Star Came To Be Known White Dwarf?" *Bulletin of the American Astronomical Society* **37**, 1503 (2005).
- [2]. S. O. Kepler, S. J. Kleinman, A. Nitta, D. Koester, B. G. Castanheira, O. Giovannini, A. F. M. Costa, and L. Althaus, "White Dwarf Mass Distribution in The SDSS," *Mon. Not. R. Astron. Soc.* **375**, 1315 (2007).
- [3]. Charles W. Misner, Kip S. Thorne, and John Archibald Wheeler, *Gravitation* (Princeton University Press, 2017).
- [4]. Hans C. Ohanian and Remo Ruffini, *Gravitation and Spacetime* (W. W. Norton & Company, 2nd ed., New York, 1994).
- [5]. Richard A. Mould, *Basic Relativity* (Springer, New York, 2002).
- [6]. Bernard F. Schutz, *A First Course In General Relativity* (Cambridge University Press, Cambridge, 1985).

- [7]. Charles Kittel and Herbert Kroemer, *Thermal Physics* (W. H. Freeman and Company, 2nd ed., San Francisco, 1980), p.196.
- [8]. Kerson Huang, *Statistical Mechanics* (John Wiley & Sons, Inc., 2nd ed., 1987), p. 247.
- [9]. Walter Greiner, Ludwig Neise, and Horst Stocker, *Thermodynamics And Statistical Mechanics* (Springer, New York, 1995), p. 359.
- [10]. J. Honerkamp, *Statistical Physics-An Advanced Approach with Applications* (Springer, 2nd ed., 2002), p.233.
- [11]. F. Schwabl, *Statistical Mechanics* (Springer, 2002), p.184.
- [12]. Koester, D. & Chanmugam, G., “Physics of White Dwarf Stars,” *Rep. Prog. Phys.* **53**, 837 (1990).
- [13]. Elvis do A. Soares, arXiv preprint arXiv:1701.02295 (2017).
- [14]. Richard D. Mattuck, *A Guide to Feynman Diagrams in the Many-Body Problem* (Dover, 2nd ed., New York, 1976), p.217.
- [15]. Gerald D. Mahan, *Many-Particle Physics* (Kluwer Academic, 3rd ed., 2000), p.297.
- [16]. F. S. Levin, *An Introiduction to Quantum Theory* (Cambridge, Cambridge, 2002), p.421.
- [17]. Roger G. Newton, *Quantum Physics* (Springer, New York, 2002), p.100.
- [18]. Stephen Gasiorowicz, *Quantum Physics* (Joh Wiley & Sons, Inc., 1974), p.185.
- [19]. Kurt Gottfried and Tung-Mow Yan, *Quantum Mechanics: Fuandamentals* (Springer, 2nd ed., 2003), p.235.
- [20]. E. E. Salpeter, “Energy And Pressure of A Zero-Temperature Plasma,” *Astrophys. J.* **134**, 669 (1961).
- [21]. Graham Woan, *The Cambridge Handbook of Physics Formulas* (Cambridge University Press, 2000, Cambridge).
- [22]. S. M. De Carvalho, M. Rotondo, Jorge A. Rueda, and R. Ruffini, “The Relativistic Feynman-Metropolis-Teller Treatment At Finite Temperatures,” *Phys. Rev. C* **89**, 015801 (2014).
- [23]. K. A. Boshkayev, J. A. Rueda, B. A. Zhami, Zh. A. Kalymova, and G. Sh. Bolgymbekov, “Equilibrium Structures of White Dwarfs At Finite Temperature,” *Int. J. Mod. Phys. Conf. Ser.* **41**, 1660129 (2016).
- [24]. G. A. Carvalho, R. M. Marinho Jr., M. Malheiro, “General Relativistic Effects In The Structure of Massive White Dwarfs,” *Gen. Relat. Gravit.* **50**, 38 (2018).
- [25]. Shoichiro Nakamura, *Applied Numerical Methods In C* (1995, Simon & Schuster (Asia) Pte. Ltd.), p.332.